THE ASTROPHYSICAL JOURNAL, 323:749–755, 1987 December 15

HIGH-EXCITATION SiO MASERS IN EVOLVED STARS

P. R. JEWELL
National Radio Astronomy Observatory[1]
DALE F. DICKINSON
Lockheed Palo Alto Research Laboratories
L. E. SNYDER
Department of Astronomy, University of Illinois
AND
D. P. CLEMENS
Steward Observatory, University of Arizona
Received 1987 March 16; accepted 1987 June 17

ABSTRACT

We report the detection of SiO maser lines from highly excited rotational states, including the $v = 1$, $J = 6$–5 transition in R Leo—the highest rotational transition detected to date. Maser emission from the $v = 1$, $J = 5$–4 transition appears to be fairly common in evolved stars, with detectability mainly determined by telescope sensitivity. Photon emission rates in the $v = 1$, $J = 5$–4 transition are typically 1–50 times less than in the $v = 1$, $J = 2$–1 transition (86 GHz). The detection of $v = 1$, $J = 6$–5 emission may be sensitivity limited, although we find evidence that the photon flux in this transition is significantly diminished relative to the lower energy transitions. VX Sgr and possibly VY CMa show $v = 2$, $J = 5$–4 emission and $v = 3$, $J = 5$–4 emission may be present in VX Sgr. In general, we find that emission from the $v = 2$ and $v = 3$ states is rare in the high rotational transitions; however SiO maser emission is largely confined to states with $v \leq 3$ and $J \leq 6$. The correlation of velocity features in the high rotational transitions with the $v = 1$, $J = 2$–1 emission features is extremely poor. Hence, theories that predict a cascade of photons within rotational ladders may have limited relevance.

Subject headings: masers — stars: circumstellar shells

I. INTRODUCTION

Maser emission from evolved stars has to date been observed from 12 rotational transitions in four vibrational states of the silicon monoxide molecule. Since these transitions arise from energy levels of ~0–5300 K above the ground state, a variety of excitation mechanisms and spatial regions may be responsible for the emission. Efforts to understand the emission have focused on comparisons between intensity, polarization characteristics, and radial velocity patterns of the different transitions and evolution of these properties with time (Schwartz, Zuckerman, and Bologna 1982; Clark *et al.* 1982; Barvainis and Predmore 1985; Snyder *et al.* 1986). Since the SiO molecule is thought to reside in an accelerating outflow (or infall) region, emission lines from different spatial locations are expected to show different radial velocities (e.g., see Moran *et al.* 1979; Elitzur 1980). Some theoretical models of SiO maser excitation have made predictions about the locations and the characteristics of emission from different states. Elitzur, Watson, and Western (1983), for example, have predicted "chains" of rotational transitions within a given vibrational state with the peak flux occurring near the central J value. Such chains would share a common radial velocity emission pattern. The more rotational states that are inverted, the greater the emission in each state. Langer and Watson (1984) expect $v = 2$ emission to occur near the photosphere in contrast to the $v = 1$ emission which they predict will originate several stellar radii away from the star. Therefore the latter should have a substantially different radial velocity pattern than the former.

It is clear from these and other theoretical efforts that a knowledge of the extent of the inversion, both vibrationally and rotationally, and the extent and correlation of the emission velocity patterns between transitions are essential to understanding the silicon monoxide maser in evolved stars. Thus, our primary purpose in these observations was to place reasonable limits on the vibrational and rotational excitation of the SiO molecule. Previous work on high rotational transitions of SiO has been performed by Schwartz, Zuckerman, and Bologna (1982), who observed $v = 1$, and $v = 2$ transitions through $J = 4$–3, and Clemens and Lane (1983), who detected $v = 1$, $J = 5$–4 emission in three stars and $v = 2$, $J = 5$–4 in one.

II. OBSERVATIONS AND DATA

The observations were performed with the NRAO 12 m telescope located on Kitt Peak, Arizona. The $J = 5$–4, $J = 6$–5, and several of the $J = 2$–1 observations were performed 1986 May 15–19, and the remaining $J = 2$–1 observations were made 1986 July 13–20. The SiO line rest frequencies were taken from Manson *et al.* (1977) and are (in MHz): $v = 1$, $J = 2$–1, 86243.350(2); $v = 1$, $J = 5$–4, 215596.035(52); $v = 1$, $J = 6$–5, 258707.489(86); $v = 2$, $J = 5$–4, 214088.594(61); $v = 3$, $J = 5$–4, 212582.560(62). The $J = 5$–4 and $J = 6$–5 SiO observations were made with cooled, dual polarization, Schottky mixer receivers operating in a double sideband mode. Position switching was employed with the off position 10′ away in azimuth. Two filter spectrometers (256 × 500 kHz and

[1] The National Radio Astronomy Observatory is operated by Associated Universities, Inc., under contract with the National Science Foundation.

TABLE 1

RESULTS OF SiO MASER OBSERVATIONS

Source (1)	α(1950) (2)	δ(1950) (3)	Transition (4)	V (LSR) (km s^{-1}) (5)	Velocity Range (km s^{-1}) (6)
Mira	2^{h}16^{m}49^{s}0	−3°12′13″	$v = 1$, $J = 2$–1	47.2	43.7–53.3
			$v = 1$, $J = 5$–4	45.0	...
			$v = 2$, $J = 5$–4	45.0	...
TX Cam	4 56 43.0	56 6 47	$v = 1$, $J = 2$–1	11.3	0.9–18.3
			$v = 1$, $J = 5$–4	8.3	3.4–13.8
			$v = 2$, $J = 5$–4	10.0	...
			$v = 1$, $J = 6$–5	10.0	...
IRC +50137	5 7 19.7	52 48 53	$v = 1$, $J = 2$–1	2.8	−0.65–6.3
			$v = 1$, $J = 5$–4	5.0	...
5 Ori	5 26 32.7	−4 43 52	$v = 1$, $J = 2$–1	12.7	8.4–17.0
			$v = 1$, $J = 5$–4	14.0	...
U Ori	5 52 51.0	20 10 5	$v = 1$, $J = 2$–1	−40.3	−43.8–−25.5
			$v = 1$, $J = 5$–4	−39.0	...
V Cam	5 55 57.5	74 30 23	$v = 1$, $J = 2$–1	7.4	−0.43–15.2
			$v = 1$, $J = 5$–4	0.0	...
IRC +60169	6 30 0.6	60 58 49	$v = 1$, $J = 2$–1	−21.3	−28.3–−17.8
			$v = 1$, $J = 5$–4	−23.5	...
VY CMa	7 20 54.7	−25 40 12	$v = 1$, $J = 2$–1	22.3	1.4–42.3
			$v = 1$, $J = 5$–4	23.1	0.8–28.6
			?$v = 2$, $J = 5$–4	−5.3	−7.4–−4.6
			$v = 1$, $J = 6$–5	21.0	...
R Leo	9 44 52.2	11 39 41	$v = 1$, $J = 2$–1	1.2	−2.3–7.1
			$v = 1$, $J = 5$–4[a]	6.2	−5.6–9.7
			$v = 2$, $J = 5$–4	1.0	...
			$v = 1$, $J = 6$–5	7.1	−0.4–9.4
R Hya	13 26 58.5	−23 1 25	$v = 1$, $J = 2$–1	−11.0	−15.3–1.2
			$v = 1$, $J = 5$–4	−8.3	−13.9–1.4
			$v = 1$, $J = 6$–5	−1.0	...
W Hya	13 46 12.2	−28 7 7	$v = 1$, $J = 2$–1	42.3	35.6–49.6
			$v = 1$, $J = 5$–4	36.2	35.5–45.9
			$v = 2$, $J = 5$–4	40.0	...
			$v = 1$, $J = 6$–5	40.0	...
RU Her	16 8 8	25 11 59	$v = 1$, $J = 2$–1	−13.2	−17.5–−7.9
U Her	16 23 34.9	19 0 17	$v = 1$, $J = 2$–1	−15.7	−20.9–−8.7
			$v = 1$, $J = 2$–1	−15.7	−20.0–−9.6
			$v = 1$, $J = 5$–4	−13.5	...
OH 2.6−0.4	17 50 10.9	−26 56 0	$v = 1$, $J = 5$–4	−4.0	...
VX Sgr	18 5 3.2	−22 14 6	$v = 1$, $J = 2$–1	8.2	−9.2–22.1
			$v = 1$, $J = 5$–4[a]	5.3	−15.6–20.6
			$v = 2$, $J = 5$–4[a]	14.1	12.0–16.1
			?$v = 3$, $J = 5$–4	17.3	...
			$v = 1$, $J = 6$–5	6.0	...
W51 IRS 2[b]	19 21 22.6	14 25 11	$v = 1$, $J = 5$–4	45.0	...
			$v = 2$, $J = 5$–4	45.0	...
χ Cyg	19 48 38.5	32 47 11	$v = 1$, $J = 2$–1	8.2	3.8–14.3
			$v = 1$, $J = 6$–5	9.5	...
NML Cyg	20 44 33.9	39 55 56	$v = 1$, $J = 5$–4	0.0	...
R Peg	23 4 8.2	10 16 21	$v = 1$, $J = 2$–1	26.0	20.8–29.5
			$v = 1$, $J = 2$–1	26.0	21.7–27.8
			$v = 1$, $J = 5$–4	17.8	13.6–18.5
			$v = 1$, $J = 6$–5	23.0	...
R Cas	23 55 51.7	51 6 35	$v = 1$, $J = 2$–1	23.8	20.4–28.2
			$v = 1$, $J = 5$–4	26.0	...

Table 1.—*continued*

	S_ν (Jy) (7)	Rms (Jy) (8)	$\int S_\nu dv$ (10^{-20} W m^{-2}) (9)	Φ_{2-1}/Φ_i (10)	1986 Date (11)	Stellar Phase (12)
Mira	758	5.4	611	...	Jul 20	0.33
	<21.9	4.4	<48.6	>31	May 16	0.19
	<16.1	3.2	<40.0	>38	May 18	0.19
TX Cam	124.0	3.5	169.0	...	Jul 15	0.33
	17.2	2.2	57.8	7.3	May 16	0.22
	<21.0	4.2	<63.2	>6.6	May 18	0.23
	<53.4	10.7	<225	>2.3	May 17	0.22
IRC +50137	20.9	2.9	19.2	...	Jul 15	...
	<20.4	4.1	<37.7	>1.3	May 17	...
5 Ori	26.4	2.4	30.3	...	Jul 15	0.45
	<30.4	6.1	<52.7	>1.4	May 16	0.31
U Ori	75.6	3.2	77.9	...	Jul 15	0.64
	<25.4	5.1	<57.8	>3.4	May 17	0.48
V Cam	51.6	4.0	81.2	...	Jul 15	0.21
	<38.9	7.8	<93.5	>2.2	May 17	0.09
IRC +60169	30.7	3.8	43.2	...	Jul 15	...
	<41.4	8.3	<94.1	>1.2	May 17	...
VY CMa	1566	8.3	3123	...	Jul 14	...
	27.3	3.4	217	36	May 16	...
	21.1	3.0	<76.2	>102	May 18	...
	<38.3	7.7	<249	>38	May 17	...
R Leo	170	5.6	196	...	Jul 13	0.80
	59.6	2.2	248	2.0	May 16	0.62
	<9.4	1.9	<21.0	>23	May 19	0.63
	41.7	5.2	162	3.6	May 18	0.62
R Hya	25.7	3.0	29.7	...	Jul 15	0.89
	39.3	2.8	131	0.6	May 16	0.74
	<54.2	10.8	<138	>0.7	May 18	0.74
W Hya	1109	10.2	1131	...	Jul 14	0.40
	81.4	3.7	236	12	May 16	0.24
	<14.1	2.8	<32.2	>87	May 19	0.25
	<41.3	8.2	<114	>30	May 18	0.24
RU Her	119.5	3.3	100	...	May 18	0.46
U Her	62.8	3.8	118	...	May 18	0.85
	87.5	5.7	137	...	Jul 15	1.00
	<12.9	2.6	<36.0	>8.2	May 16	0.85
OH 2.6−0.4	<19.2	3.8	...	...	May 16	...
VX Sgr	422.2	2.8	1307	...	May 18	...
	17.2	1.7	123	26	May 16	...
	31.2	3.7	50.1	65	May 19	...
	7.5	1.5	...	...	May 19	...
	<39.4	7.9	<209	>19	May 17	...
W51 IRS 2[b]	<18.2	3.6	...	...	May 16	...
	<6.90	1.4	...	...	May 19	...
χ Cyg	254.6	3.1	263	...	May 18	0.76
	<31.9	6.4	<75.9	> 10	May 18	0.76
NML Cyg	<31.1	6.2	...	...	May 16	...
R Peg	53.0	3.1	52.7	...	May 18	0.06
	37.4	3.6	44.5	...	Jul 15	0.22
	8.0	1.8	15.1	8.7	May 16	0.06
	<18.6	3.7	<44.4	>3.6	May 17	0.06
R Cas	389	4.0	299	...	May 18	0.86
	<26.4	5.3	<46.3	>16	May 16	0.86

[a] This emission was previously detected by Clemens and Lane 1983.
[b] A possible line in W51 IRS 2 was detected at 214060 MHz with an intensity of ~0.10 K. This is probably background emission from an unidentified species.

256 × 1 MHz) were used in parallel. Each filter bank was divided into halves, with each half accepting an orthogonal linear polarization channel. The spectra and tabular results reported here are an average of the two polarization channels. The 1.5 GHz IF frequency of the receiver allowed the $v = 1$ and $v = 3$ $J = 5$–4 lines to be observed simultaneously, with one in the upper sideband and the other in the lower.

The data were calibrated by the chopper wheel technique which corrects for atmospheric attenuation and antenna spillover losses and results in temperatures expressed on the T_R^* scale (Kutner and Ulich 1981). The effective system temperature, T_{sys}^*, which results from the calibration scale was 1200–1500 K at the $J = 5$–4 frequency and 2500–3000 K at the $J = 6$–5 frequency. The flux density scale was set by observations of Jupiter. The conversion factor from T_R^* to flux density was 53 Jy K^{-1} at the $J = 5$–4 frequency and 80 Jy K^{-1} at the $J = 6$–5 frequency. The FWHP of the antenna beam was 32″ at the $J = 5$–4 frequency and 26″ at the $J = 6$–5 frequency as determined by five point maps of Saturn.

The $J = 2$–1 observations were made with a 3 mm cooled, dual polarization, Schottky receiver. The observing technique was identical to the higher frequency observations except that the filter spectrometers used were 100, 250, or 500 kHz per channel. The FWHP was 70″ at the $J = 2$–1 line. T_{sys}^* was 750–1000 K, and the conversion from T_R^* to flux density was 32 Jy K^{-1}.

Table 1 summarizes the results of the high J observations and the associated $v = 1$, $J = 2$–1 observations. Source names, coordinates, and transition quantum numbers are given in the first four columns. The next two columns list V(LSR), the radial velocity with respect to the local standard of rest of the strongest emission feature, and the velocity range of all detectable emission. The next three columns contain S_v, the peak flux density of the strongest emission feature which was identified in the V(LSR) column; rms, the root mean square noise level of the spectrum; and $\int S_v\,dv$, the flux density integrated over the velocity range listed in the sixth column. The next column contains Φ_{2-1}/Φ_i, the ratio of photon flux in the $v = 1$, $J = 2$–1 transition to the photon flux of the transition listed in the fourth column. The last two columns list the dates of observation and the stellar phases at those epochs, if that information was available. The phase information was obtained from the American Association of Variable Star Observers (Mattei 1986*a*, *b*) and the *General Catalogue of Variable Stars* (Kukarkin *et al.* 1969). Figures 1–7 present the high-excitation lines along with their $J = 2$–1 counterparts for the seven detections.

III. DISCUSSION

a) Emission Characteristics

Figure 1 shows the $v = 1$, $J = 6$–5 spectrum of SiO in R Leo together with the $v = 1$, $J = 5$–4 and the $v = 1$, $J = 2$–1 spectra. The features at 2.4 and 6.5 km s^{-1} in the $J = 6$–5 spectrum correspond well in velocity with two prominent features in the $J = 5$–4 spectrum. However, the high J profiles do not correspond at all with the $J = 2$–1 profile. the $J = 5$–4 profile actually has a substantially larger width than the other transitions. These profiles suggest that maser cascade chains might occur over a few levels, but the correlation between the upper and lower members of the ladder eventually breaks down. We note that the $J = 2$–1 observation was made 2 months after the high J observations. Clark *et al.* (1984) have

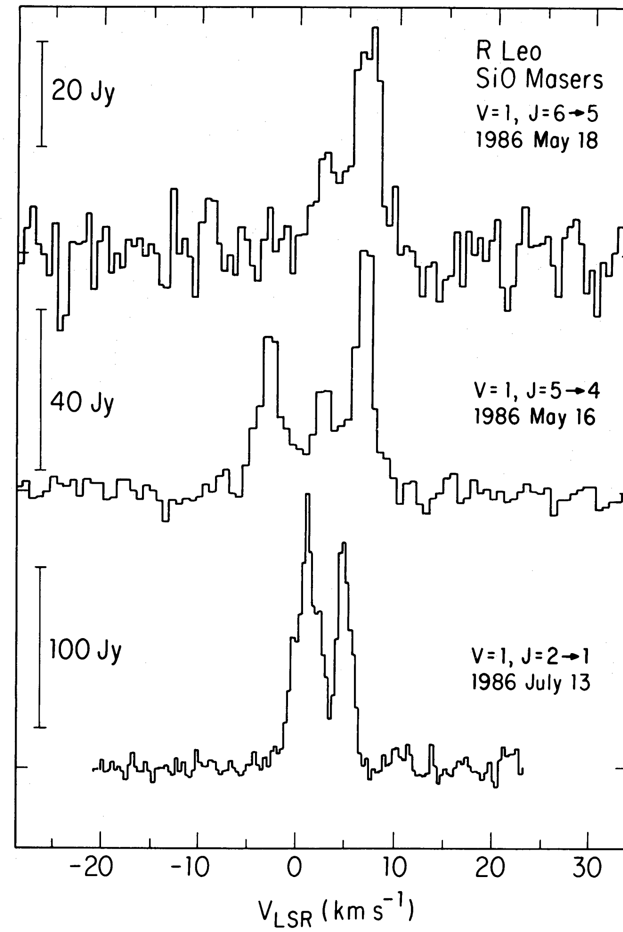

FIG. 1.—R Leo SiO masers in the $v = 1$, $J = 6$–5 (258707.489 MHz), $v = 1$, $J = 5$–4 (215596.035 MHz), and $v = 1$, $J = 2$–1 (86243.350 MHz) transitions. The $J = 6$–5 maser is the highest frequency SiO maser yet detected. The stellar phase was 0.62 for the 1986 May observations and 0.80 for the 1986 July observation.

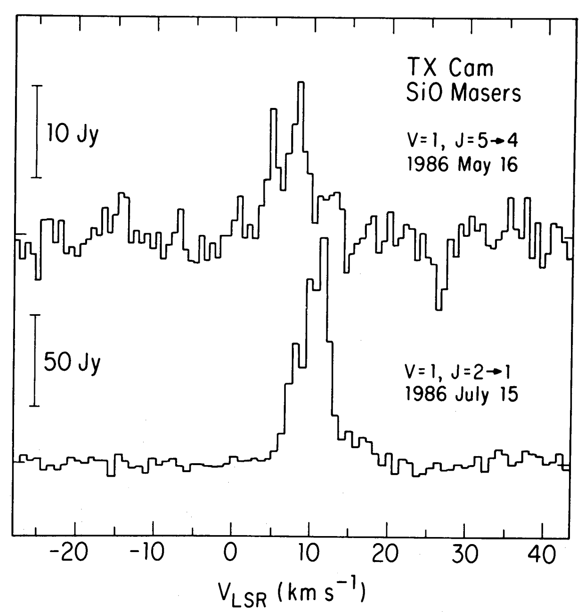

FIG. 2.—TX Cam SiO masers in the $v = 1$, $J = 5$–4 and $v = 1$, $J = 2$–1 transitions. The stellar phase was 0.22 for the 1986 May observation and 0.33 for the 1986 July observation.

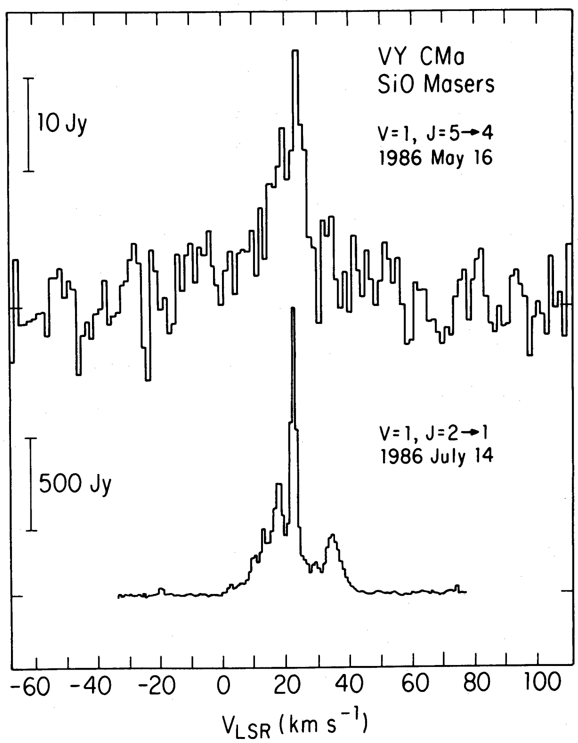

FIG. 3.—VY CMa SiO masers in the $v = 1$, $J = 5$–4 and $v = 1$, $J = 2$–1 transitions. Stellar phase information was not available for this source.

shown that SiO maser emission characteristics can undergo significant changes shortly after stellar maximum. Emission properties (intensity, velocity pattern) can show more uniform changes throughout the stellar cycle (e.g., Lane 1982; Clark *et al.* 1984). R Leo was at phases 0.62 and 0.80 at the two dates of observations, so it probably did not experience radical changes.

Figure 2 shows the $J = 5$–4 and $J = 2$–1 emission from TX Cam. The $J = 5$–4 emission lies within the velocity range of the $J = 2$–1 emission complex, but the strongest features do not coincide in velocity. Figure 3 shows the $J = 5$–4 and $J = 2$–1 emission from VY CMa. This is one of only two sources showing good velocity correspondence between the $J = 5$–4 and $J = 2$–1 emission. Figure 4 shows the $J = 5$–4 and $J = 2$–1 emission from R Hya. This source is remarkable since the photon flux of the $J = 5$–4 (May 16) actually exceeds the $J = 2$–1 photon flux (July 15). We did not detect $J = 6$–5 emission, however. R Hya was at phases 0.74 and 0.89 at the two dates of observation. Strong emission occurs near -11 km s^{-1} in both transitions. Figure 5 shows the $J = 5$–4 and $J = 2$–1 emission from W Hya. The emission complexes cover a similar velocity interval, but the prominent velocity features in each transition do not correspond. Figure 6 shows the VX Sgr $J = 5$–4 emission spectra in the $v = 1$ state (and possibly the $v = 3$ state) and the $v = 2$ state, followed by the $v = 1$, $J = 2$–1 emission spectrum. The $v = 3$, $J = 5$–4 feature was in the lower sideband of all the $v = 1$, $J = 5$–4 upper sideband observations, and, if our suggested assignment is correct, it would be the highest excitation maser known. However, VX Sgr is near the galactic plane so we cannot absolutely rule out the possibility that this feature could be background emission from an unknown species. Moreover, our method of data averaging was referenced to only the upper sideband so any lower sideband $v = 3$ line would be artificially broadened and reduced in intensity. The spectrum in the small inset was obtained by properly averaging the data for the lower sideband, so it shows the correct width and intensity for the possible $v = 3$ feature. All the $J = 5$–4 emission falls within the $J = 2$–1 emission interval, but none of the prominent emission features align in velocity. The $J = 5$–4 line intensities for VX Sgr are more

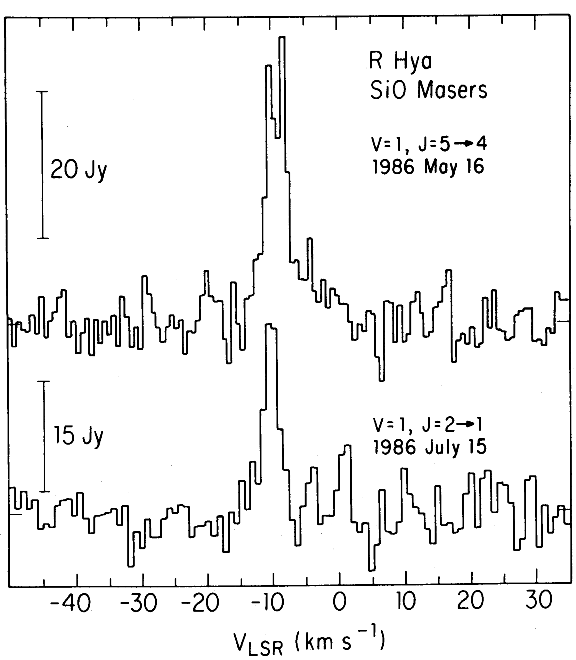

FIG. 4.—R Hya SiO masers in the $v = 1$, $J = 5$–4 and $v = 1$, $J = 2$–1 transitions. The stellar phase was 0.74 for the 1986 May observation and 0.89 for the 1986 July observation.

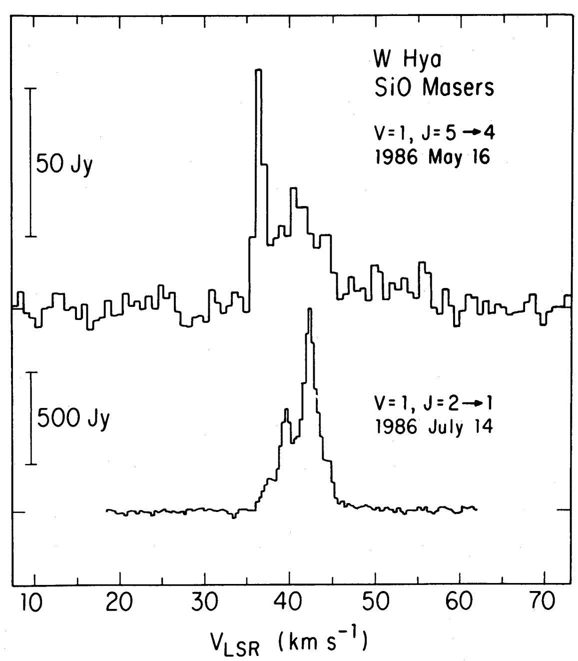

FIG. 5.—W Hya SiO masers in the $v = 1$, $J = 5$–4 and $v = 1$, $J = 2$–1 transitions. The stellar phase was 0.24 for the 1986 May observation and 0.40 for the 1986 July observation.

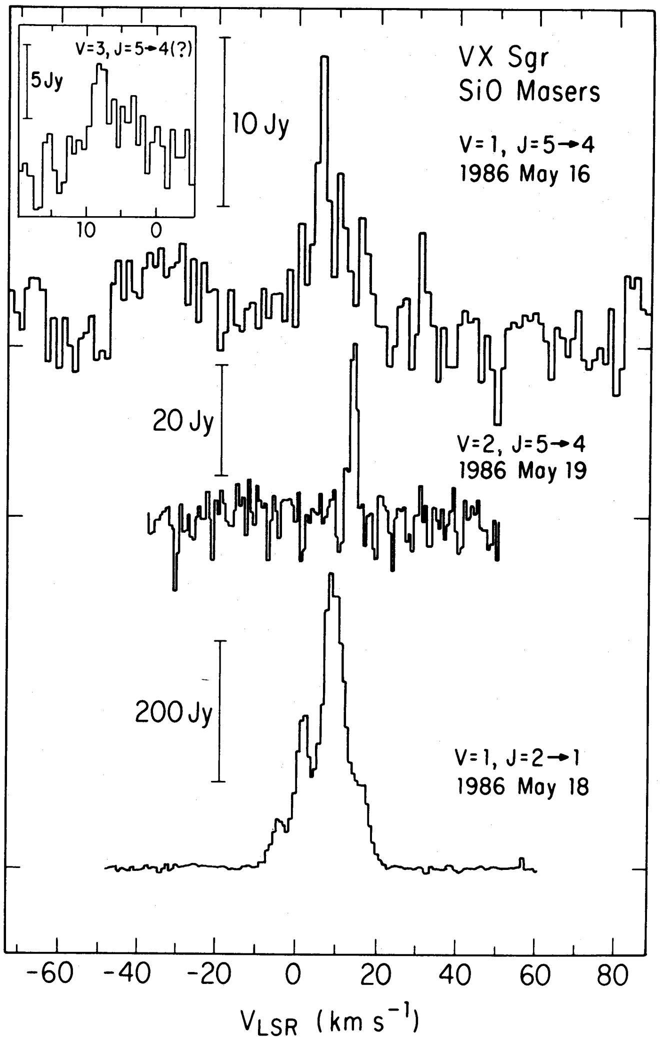

FIG. 6.—VX Sgr SiO masers in the $v = 1$, $J = 5$–4, $v = 2$, $J = 5$–4, and $v = 1$, $J = 2$–1 transitions. The feature in the $v = 1$, $J = 5$–4 upper sideband spectrum at an apparent velocity of -35 to -45 km s^{-1} is the suspected $v = 3$, $J = 5$–4 emission from the lower sideband which has been broadened and reduced in intensity from local oscillator shift alignments for the upper sideband. The spectrum in the small inset was obtained by properly averaging the data for the lower sideband to show the proper width and intensity for the possible $v = 3$ feature. Stellar phase information was not available for this source.

uncertain than for the other sources because of disagreement in the literature over the best source coordinates. The VX Sgr $J = 2$–1 emission was mapped for peak intensity, but the $J = 5$–4 emission, which was observed with a different receiver configuration, was too weak to map. Figure 7 shows the $J = 5$–4 and $J = 2$–1 emission from R Peg. Again, little correspondence between the strongest velocity features exists.

Only upper limits were obtained for the $v = 1$, $J = 5$–4 emission from Mira (*o* Ceti), IRC +50137, S Ori, U Ori, V Cam, IRC +60169, S CrB, U Her, OH 2.6−0.4, W51 IRS 2, NML Cyg, and R Cas. Most of these sources are weaker in the $J = 2$–1 line than are those that produced positive results. The limit on the photon flux ratio Φ_{2-1}/Φ_{5-4} ranged from 1 to 31 for the nondetections. The upper limit on integrated flux density, from which photon flux is derived, was defined as $5\sigma\Delta\nu_{2-1}/\sqrt{N}$, where σ is the rms noise of the transition of interest, $\Delta\nu_{2-1}$ is the frequency width of the $v = 1$, $J = 2$–1 emission, and N is the number of channels in the frequency interval. Two of the sources listed above, Mira and R Cas, are strong in the $J = 2$–1 line. The photon flux ratio Φ_{2-1}/Φ_{5-4} is greater than 31 for Mira and greater than 16 for R Cas.

Figure 8 is a plot of $v = 1$, $J = 5$–4 flux density versus $v = 1$, $J = 2$–1 flux density. This plot provides three notable results: (1) the Mira sources have a large scatter in their $J = 5$–4 to $J = 2$–1 flux density ratios, suggesting that this particular SiO emission characteristic is strongly influenced by random events; (2) the two supergiants, VX Sgr and VY CMa, lie close to a line through zero flux and may thus have a more regular behavior in flux density ratios, although the statistics indicating this trend are obviously small; (3) the points all lie in the upper diagonal of the plot, which suggests that $S_\nu[J = 5\text{–}4] \geq (1/15)S_\nu[J = 2\text{–}1]$.

Upper limits for $v = 1$, $J = 6$–5 emission were obtained for TX Cam, VY CMa, R Hya, W Hya, VX Sgr, χ Cyg, and R Peg. For the sources VY CMa, W Hya, and VX Sgr, all of which have strong $v = 1$, $J = 2$–1 and $v = 1$, $J = 5$–4 emission, limits on $\Phi_{2-1}/\Phi_{6-5} > 19$–38 were obtained. Upper limits were also obtained for $v = 2$, $J = 5$–4 emission from Mira, TX Cam, R Leo, W Hya, and W51 IRS 2. Hasegawa *et al.* (1986) have reported $v = 2$, $J = 1$–0 emission from the vicinity of W51 IRS 2, a star-forming region. The lower bounds on the $v = 2$, $J = 2$–1 and $v = 2$, $J = 5$–4 photon flux ratio ranged from 7 to 100. With the exception of VX Sgr, no evidence of $v = 3$ emission was seen.

IV. CONCLUSIONS

1. From the six detections, we conclude that the $v = 1$, $J = 5$–4 SiO maser is fairly common. Considerable variation from star to star occurs, but the photon flux ratio Φ_{2-1}/Φ_{5-4} is typically 1–50. Most of the strongest $J = 2$–1 sources showed $J = 5$–4 maser emission as well—Mira and R Cas were exceptions. From detections and nondetections, we find the possible relation $S_\nu[J = 5\text{–}4] \geq (1/15)S_\nu[J = 2\text{–}1]$. As the sensitivity of telescopes improves, probably many new $v = 1$, $J = 5$–4 maser sources will be discovered.

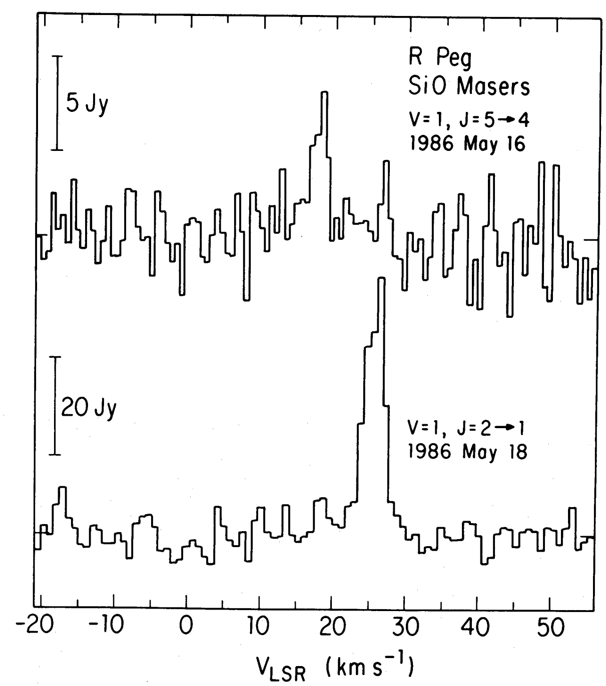

FIG. 7.—R Peg SiO masers in the $v = 1$, $J = 5$–4 and $v = 1$, $J = 2$–1 transitions. The stellar phase was 0.06 for these observations.

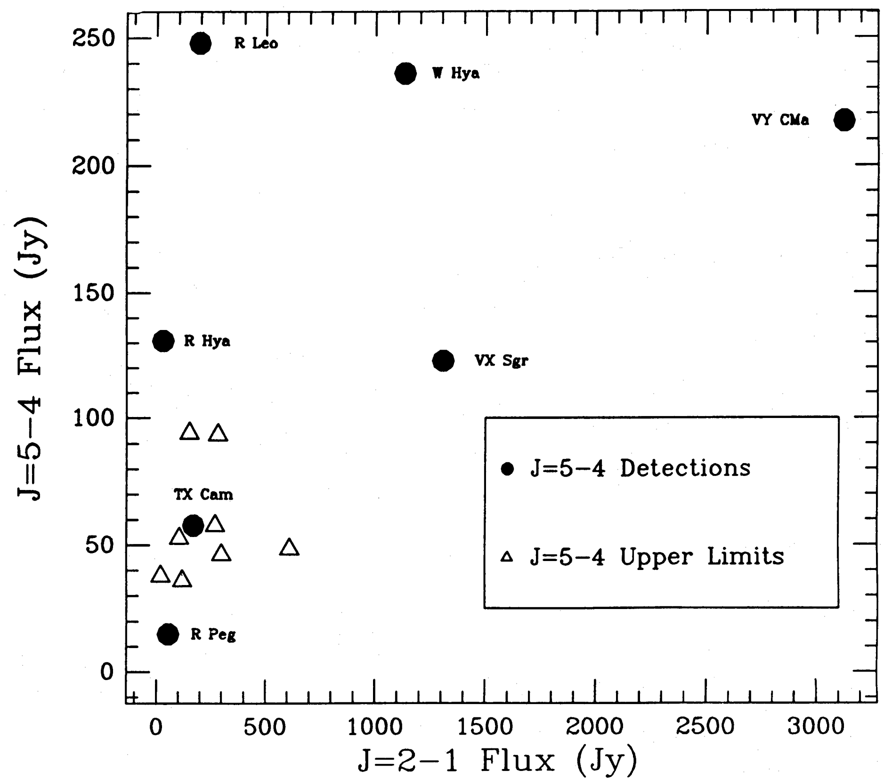

FIG. 8.—Flux-flux plot of observed $v = 1, J = 5$–4 vs. $v = 1, J = 2$–1 flux densities. Data were taken from Table 1.

2. At present sensitivities, maser emission in the $v = 1$, $J = 6$–5 transition is rare; the excitation of this transition is significantly diminished relative to lower lying transitions. R Leo showed relatively strong $J = 6$–5 maser emission, but upper limits on $J = 6$–5 in VY CMa, W Hya, and VX Sgr were stringent. These latter three sources all had strong $J = 5$–4 lines. In general, SiO maser excitation appears to be confined to $v \leq 3$ and $J \leq 6$.

3. The observations of this study do not support theories advocating a cascade of photons down the entire SiO rotational ladder. Four of the six detections showed little similarity in the velocity profiles of the $J = 5$–4 and $J = 2$–1 transitions (all of the observations were made within a 2 month time period). The $J = 5$–4 and $J = 6$–5 profiles in R Leo had some similarity, however, which suggests that maser chains might exist over a few levels. Barvainis and Predmore (1985) have also found little correspondence between velocity and polarization features of $J = 1$–0 and $J = 2$–1 masers.

The authors thank the 12 m telescope operators, Dennis Chase and Werner Scharlach, for their assistance in these observations, and J. A. Mattei of the AAVSO for providing stellar phase information. L. E. S. acknowledges past support from NSF grant AST-8217547 to the University of Illinois. D. P. C. acknowledges partial support by a Cottrell Research Grant from the Research Corporation.

REFERENCES

Barvainis, R., and Predmore, C. R. 1985, *Ap. J.*, **288**, 694.
Clark, F. O., Troland, T. H., and Johnson, D. R. 1982, *Ap. J.*, **261**, 572.
Clark, F. O., Troland, T. H., Pepper, G. H., and Johnson, D. R. 1984, *Ap. J.*, **276**, 572.
Clemens, D. P., and Lane, A. P. 1983, *Ap. J.* (*Letters*), **266**, L117.
Elitzur, M. 1980, *Ap. J.*, **240**, 553.
Elitzur, M., Watson, W. D., and Western, L. R. 1983, *Ap. J.*, **274**, 210.
Hasegawa, T., Morita, K., Okumura, S., Kaifu, N., Suzuki, H., Ohishi, M., Hayashi, M., and Ukita, N. 1986, in *Masers, Molecules, and Mass Outflows in Star Forming Regions*, ed. A. D. Haschick (Westford, MA: Haystack Observatory), p. 275.
Kukarkin, B. V., *et al.* 1969, *General Catalogue of Variable Stars* (3rd ed.; Moscow: Astr. Council USSR).
Kutner, M. L., and Ulich, B. L. 1981, *Ap. J.*, **250**, 341.
Lane, A. P. 1982, Ph.D. thesis, University of Massachusetts.
Langer, S. H., and Watson. W. D. 1984, *Ap. J.*, **284**, 751.
Manson, E. L., Jr., Clark, W. W., De Lucia, F. C., and Gordy, W. 1977, *Phys. Rev.*, **15**, 223.
Mattei, J. A. 1986*a*, private communication.
———. 1986*b*, *American Association of Variable Star Observers*, Bull. No. 49.
Moran, J. M., *et al.* 1979, *Ap. J.* (*Letters*), **231**, L67.
Schwartz, P. R., Zuckerman, B., and Bologna, J. M. 1982, *Ap. J.* (*Letters*), **256**, L55.
Snyder, L. E., Jewell, P. R., Dinger, A. S., Dickinson, D. F., and Buhl, D. 1986, *A.J.*, **92**, 416.

DAN P. CLEMENS: Steward Observatory, Campus Building 65, 949 North Cherry Avenue, Tucson, AZ 85721-0655

DALE F. DICKINSON: Code 92-20, Lockheed Palo Alto Research Laboratory, 3251 Hanover Street, Palo Alto, CA 94304

PHILIP R. JEWELL: National Radio Astronomy Observatory, Campus Building 65, 949 North Cherry Avenue, Tucson, AZ 85721-0655

LEWIS E. SNYDER: Astronomy Department, University of Illinois, 341 Astronomy Building, 1011 West Springfield Avenue, Urbana, IL 61801-3000